Experimental Study on Influence of Different Pile Installation Methods on Performance of Pile

Mako AIZAWA
Student, Kanazawa University, Kanazawa, Japan
Tatsunori MATSUMOTO
Professor, Graduate School of Kanazawa University, Kanazawa, Japan
Email: matsumoto@se.kanazawa-u.ac.jp
Shunsuke MORIYASU
Senior Researcher, Nippon Steel & Sumitomo Metal Corp., Tokyo, Japan
Soichiro SUKO
Graduate student, Graduate School of Kanazawa University, Kanazawa, Japan
Shun-ichi KOBAYASHI
Associate Professor, Graduate School of Kanazawa University, Kanazawa, Japan
Shinya SHIMONO
Technician, Kanazawa University, Kanazawa, Japan

ABSTRACT

In this research, penetration resistance and load-settlement relations of a pile installed by jack-in, surging and vibratory were investigated through model tests in dry or saturated sand grounds. An open-ended aluminum pipe having a length L of 597 mm, an outer diameter D_o of 32.0 mm and an inner diameter D_i of 29.3 mm was used for the model pile. The model pile was instrumented with axial strain gauges at 5 cross-sections to obtain axial forces in the pile. The model ground was dry or saturated silica sand in a cylindrical container having a diameter of 566 mm and a height of 540 mm. Relative densities D_r of the dry and saturated grounds were 80% and 70%, respectively. In the case of the saturated ground, 7 pore water pressure transducers were buried in the model ground at different depths and different horizontal distances from the pile. In each experiment, the model pile was first installed into the model ground by jack-in or surging or vibratory to a depth of about 400 mm. After the installation process, a static load test (SLT) was carried out, in order to compare the load-settlement behaviours of the pile installed by the three different methods.

Key words: *Pile installation method, Press-in, Vibratory, Sand, Pore water pressure*

1. Introduction

Various operational techniques are available for facilitating penetration of displacement piles, for examples, impact pile driving, jack-in, surging (repetition of push-in and pull-out strokes) and vibratory driving. It was widely recognised that a displacement pile has higher bearing capacity than a non-displacement pile even if they have the same configuration.

Recently, it is rather difficult to employ pile driving technique especially in urban areas, because of environmental problems such as noises and severe ground vibrations associated with pile driving. Press-in (jack-in) technologies including surging and vibratory techniques have been developed.

However, it has not been quantitatively understood how behaviours of a pile during and after pile installation are affected by different piling methods and ground conditions.

The purpose of this research is to investigate influences of different piling methods and ground

conditions on pile behaviours, such as penetration resistance, load-settlement relation and bearing capacity. In this particular paper, penetration resistance and load-settlement relations of a pile installed by jack-in, surging and vibratory were investigated through model tests in dry or saturated sand grounds.

2. Description of the experiments

The experimental devices and procedure in the research are similar to those in Moriyasu *et al.* (2016) where experiments in dry sand ground only were carried out. In this research, experiments in saturated sand ground were added, because the ground water exists in the field.

2.1. Model pile

An open-ended aluminum pipe having a length, L, of 597 mm, an outer diameter, D_o, of 32.0 mm and an inner diameter, D_i, of 29.3 mm was used for the model pile. **Fig. 1** shows configuration, and physical and mechanical properties of the model pile. The model pile was instrumented with axial strain gauges at 5 cross-sections to obtain axial forces in the pile.

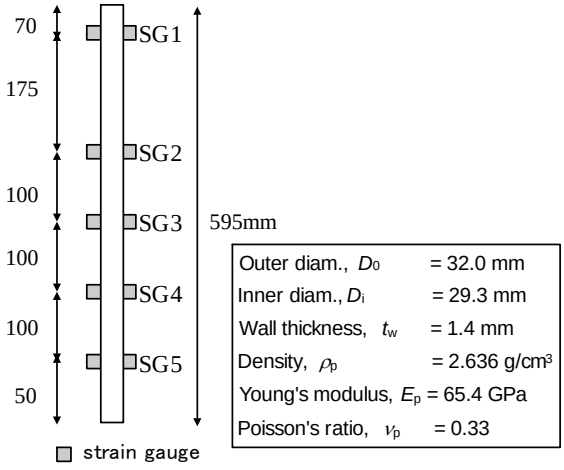

Fig. 1 The model pile

2.2. Model ground

Model ground was dry or saturated silica sand in a cylindrical container having a diameter of 566 mm and a height of 580 mm as shown in **Fig. 2**. Silica No.6 was used in experiments. The physical properties of silica No.6 are listed in **Table 1**. In the case of the dry ground, the sand was poured into the soil box in a thickness of about 50 mm, and was tamped so that each layer had a relative density, D_r, of 80%. This procedure was repeated until the height of the model ground reached 580 mm. In the case of the saturated ground, the soil box was filled with de-aired water first, then the dry wand was poured into the soil box in layers and tamped aiming at that D_r of the model ground had D_r = 80%. However, D_r of the saturated grounds ranged from 65% to 70%, because of a difficulty of compaction by tamping.

In the cases of the saturated ground, 7 pore water pressure transducers were buried in the model ground at different depths and different horizontal distances from the pile.

Table 1. Physical properties of silica No.6

Soil particle density, ρ_s (t/m^3)	2.679
Min. dry density, ρ_{dmin} (t/m^3)	1.366
Max. dry density, ρ_{dmax} (t/m^3)	1.629
Max. void ratio, e_{max}	0.962
Min. void ratio, e_{min}	0.645
Average particle size, D_{50}	0.52

Fig. 2 A saturated model ground

2.3. Experimental procedure and cases

In each experiment, the model pile was first installed into the model ground by jack-in or surging (repetition of downward movement of 2 mm and upward movement of 1 mm) or vibratory to a depth of about 400 mm. In the cases of jack-in and surging, the pile head force was measured via a load cell placed on the pile top. A vibratory hammer (**Fig. 3**) was used in the cases of vibratory penetration.

Two electric motors having eccentric mass were rotated in opposite wise-directions synchronously to apply vertical force on the pile head. The acceleration at the pile head was measured in the case of vibratory installation.

After the installation process, static load test (SLT) was carried out, in order to compare the load-settlement behaviours of the pile installed by the 3 different methods. Height of the soil plug inside the pipe pile was measured after the completion of the SLT. Cone Penetration Tests (CPTs) were conducted at several locations in the model ground in each experiment to check the repeatability of the model grounds. Experimental cases and conditions are listed in **Table 2**.

Fig. 4 shows vertical the theoretical effective stresses with depth in the case of dry and saturated grounds. Note that ground water levels in Cases 4 and 6 were 100 mm blow the ground surface. **Fig. 5** shows the CPT results for Case 2 (dry sand) and Case 5 (saturated sand). CPT results of the other dry and saturated grounds were similar to **Fig. 5**. It is seen that CPT tip resistance, σ_{tip}, in the saturated ground was smaller than that in the dry ground due to smaller effective vertical stresses in the saturated ground.

Table 2. Experimental cases and conditions

Case No.	1	2	3	4	5	6
Model ground	Dry	Dry	Dry	Saturated	Saturated	Saturated
Relative density, D_r (%)	79.9	79.9	80	69.5	64.3	69.5
Dry density, ρ_d (t/m^3)	1.568	1.568	1.568	1.538	1.524	1.538
Penetration method in PPT	Push-in	Surging	Vibration	Push-in	Surging	Vibration
Penetration speed (mm/s)	0.2	0.2	-	0.2	0.2	-
Vibration frequency (Hz)	-	-	20Hz to 35Hz	-	-	15Hz to 20Hz
Test sequence	PPT ↓ SLT ↓ CPT	PPT ↓ SLT ↓ CPT	Static loading by V.H. weight ↓ Vibratory Penetration ↓ SLT ↓ CPT	PPT ↓ SLT ↓ CPT	PPT ↓ SLT ↓ CPT	Static loading by V.H. weight ↓ Vibratory penetration ↓ SLT ↓ CPT

PPT: Pile Penetration Test, SLT: Static Loading Test, CPT: Cone Penetration Test, V.H.: Vibratory Hammer

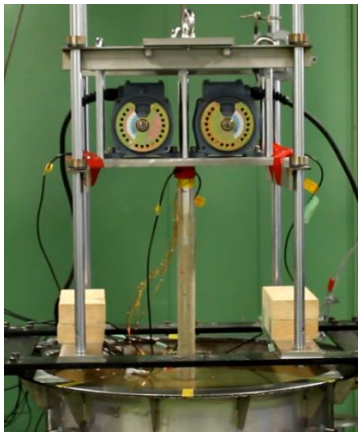

Fig. 3 Vibratory hammer

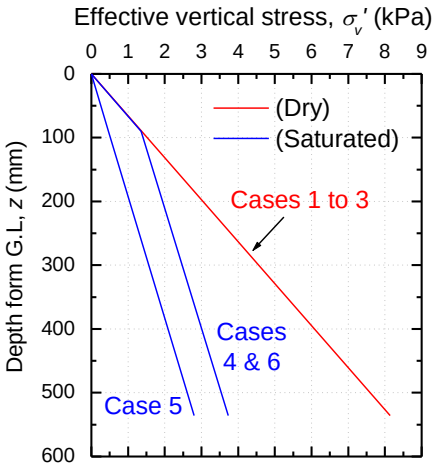

Fig. 4 Vertical effective stress

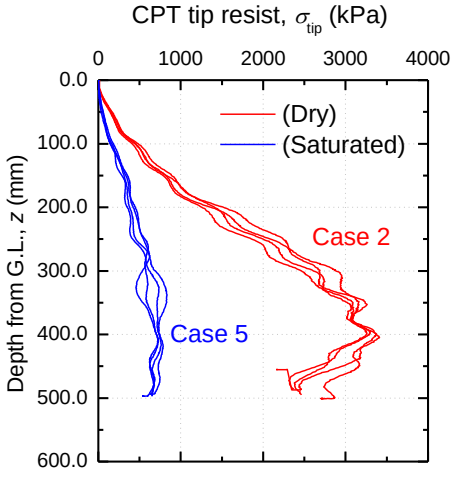

Fig. 5 CPT results

2.4. Consolidated-undrained shear tests of the sand

Consolidated-undrained monotonic and cyclic shear tests were conducted to investigate the mechanical behaviour of the silica No. 6, because an undrained condition of the saturated ground was expected during the vibratory driving.

Fig. 6 shows the relationship between the axial strain, $\varepsilon_{a,,}$ and the deviatoric stress, q. **Fig. 7** shows the relationship between ε_a and the excess pore water pressure, u_e. **Fig. 8** shows the effective stress paths. In those tests, confining pressure was about 30 kPa. Internal frictional angle of the sand is 38 to 40 degrees, and phase angle is 25 degrees.

It is seen from **Fig. 6(b)** that ε_a increases with number of cyclic loadings with each constant q. Excess pore water pressure generated in the cyclic shear test was greater than that in the monotonic shere test (**Fig. 7(b)**). It is also seen that the excess pore water pressure increased with the number of cyclic loading. After the cyclic loading stage, the beheviours of the sand in both tests were similar.

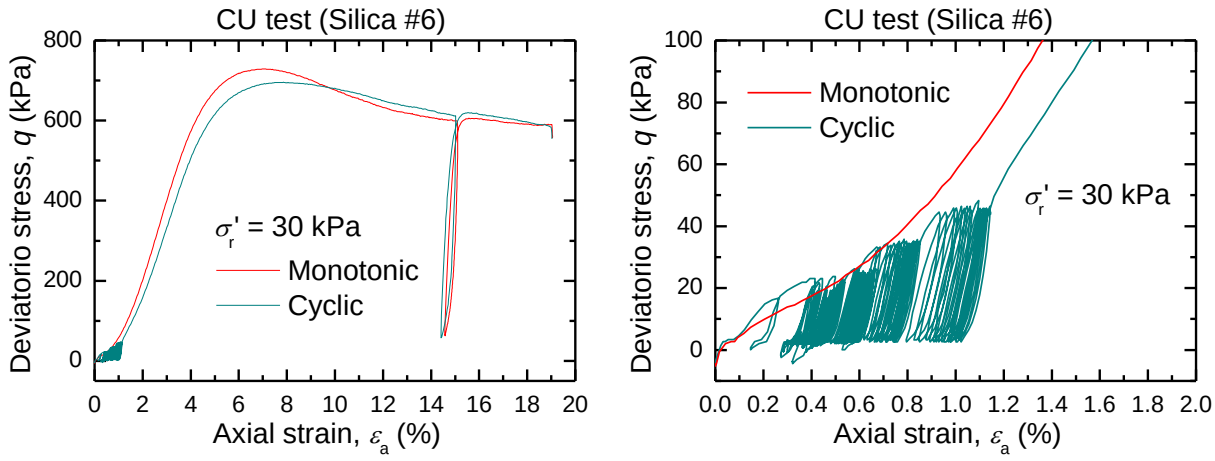

(a) General view **(b)** Enlarged view

Fig. 6 The relationship between the axial strain, $\varepsilon_{a,,}$ and the devlatoric stress, q

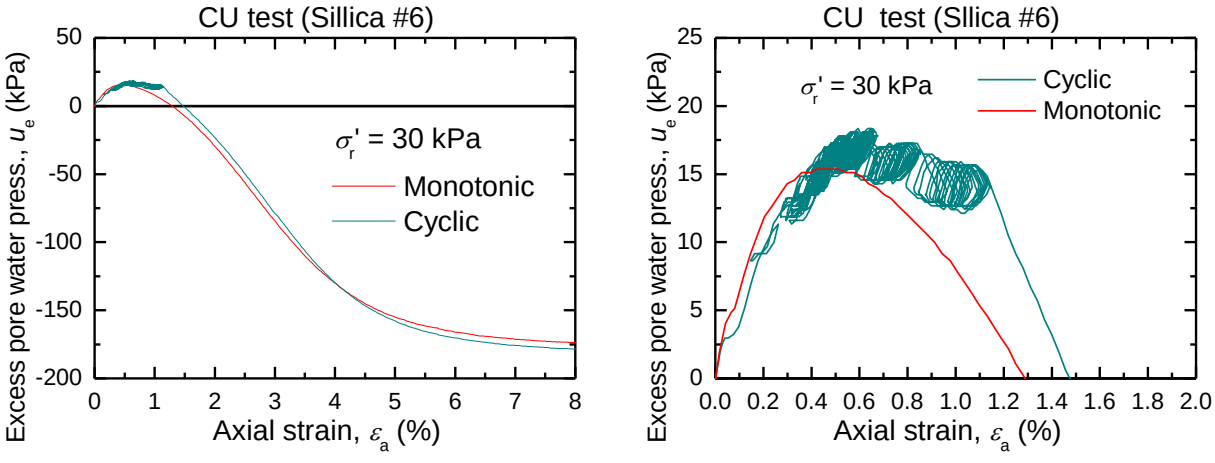

(a) General view **(b)** Enlarged view

Fig. 7 The relationship between the axial strain, ε_a, and the excess pore water pressure, u_e

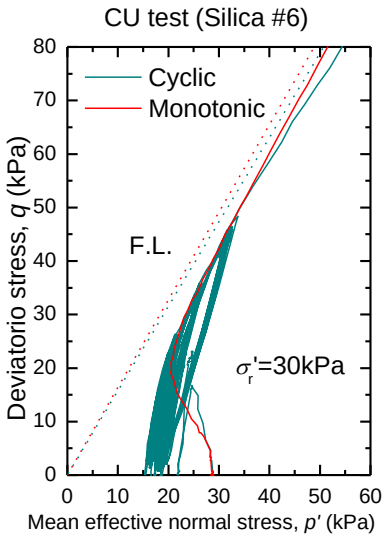

Fig. 8 Effective stress paths

3. Results of pile loading experiments

The results of various pile loading experiments are presented in this section. As mentioned in Section 2, the ratio of the pile radius and the radius of the soil box was about 18. It may be judged that the influence of the lateral boundary of the soil box on the pile behaviour is negligible in the cases of static loading, such as push-in and surging tests.

On the other hand, in the case of vibratory driving, the waves travelling in the model ground horizontally are reflected at the lateral wall of the soil box. This condition is quite different from the practice where the ground extends infinitely in the horizontal direction. Furthermore, in the cases of static loading in the saturated ground, the drainage boundary conditions of the model ground and the practical ground are quite different. That is, the lateral wall of the soil box is the impermeable boundary in the horizontal direction, while the impermeable boundary in the horizontal direction does not exist in the field.

Hence, the experimental results of the vibratory driving may not representative for that in the field. However, the results may be indicative of the influence of the vibratory driving in the limited experimental conditions in this study.

3.1. Pile penetration stage

Fig. 9 shows the relationship between the pile head load, P_h, and the pile head displacement, w_h, in Cases 1 to 3 in the cases of the dry ground. It can be seen that P_h in Case 1 and Case 2 during PPT (Pile Penetration Test) are almost similar. In Case 3, P_h is considerably small compared to those in Case 1 and Case 2 during PPT.

Fig. 10 shows the relationship between P_h and w_h in Cases 4 to 6 of the saturated ground. During PPT, P_h in Case 5 (surging) is slightly smaller than P_h in Case 4 (push-in). In Case 6, frequency, f, of the vibro-hammer gradually increased depending on degradation of penetrability. P_h in Case 6 have been a little bit smaller than that in Case 5, or almost the same as that in Case 5 until f increased to 17.7 Hz. When f increased to 18.3 Hz, P_h drastically decreased.

In general, the pile head load, P_h, in each pile installation method in the dry ground are higher than those in the saturated ground. This may be attributed to the higher effective vertical stresses in the dry ground (see **Fig. 4)**. This effect is also seen in the difference of the cone tip resistance between the dry and the saturated grounds (see **Fig. 5**).

Fig. 11 shows locations of 7 pore water pressure transducers in Cases 4 to 6. **Fig. 12** shows the relationship between the pile head displacement, w_h, and the water pressure (P.W.P.), p, during PPT. **Fig. 13** shows the relationship between w_h and p, in SLT. It can be seen in **Fig. 12(c)** that pore water pressures increased rapidly when the pile tip reached a depth of 400 mm. It is noted that at this depth the frequency, f, of the V.H. increased from 17.7 Hz to 18.3 Hz, because more pile penetration was difficult with f = 17.7 Hz. Just after f increased to 18.8 Hz, P_h increased and the pile started to penetrate again (see **Fig. 10(c)**). However, as mentioned above, pore water pressures increased rapidly when the pile tip reached the depth of 400 mm, resulting in the penetration resistance of the pile, P_h, dramatically decreased.

The increased water pressures and the initial overburden stresses indicate that the model ground was liquefied when the pile tip reached the depth of 400 mm due to increasing the frequency of V.H. to 18.3 Hz. It can be said that fully-undrained condition was achieved with f = 18.3 Hz.

The consolidated-undrained shear tests shows that higher positive excess pore water pressure was generated in the cyclic test than in the monotonic test (**Fig. 7**). And these tests show that effective stress was smaller in the cyclic test than in the monotonic test (**Fig. 8**).

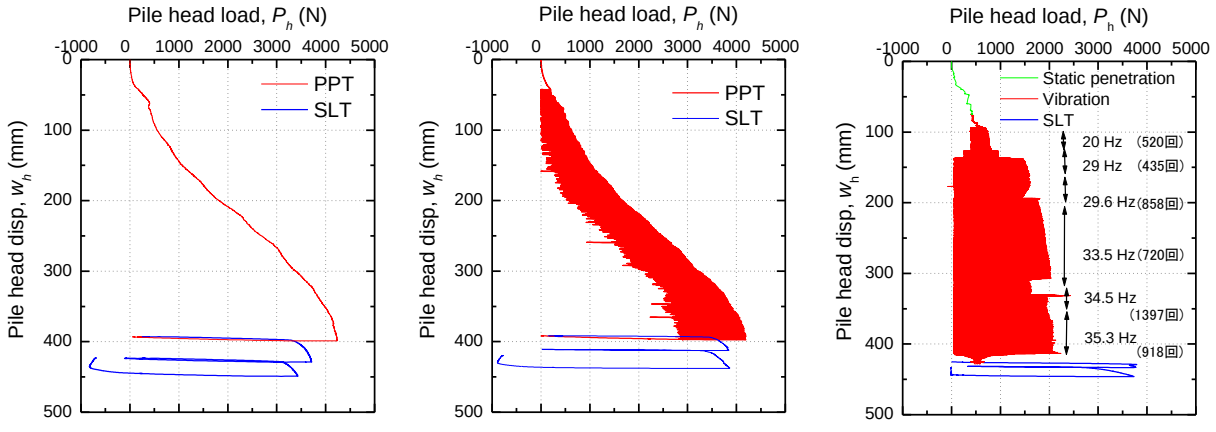

(a) Case 1 (Dry, Push-in) **(b)** Case 2 (Dry, Surging) **(c)** Case 3 (Dry, Vibratory)

Fig. 9 The relationship between the pile head load, P_h, and the pile head displacement, w_h, in Cases 1 to 3

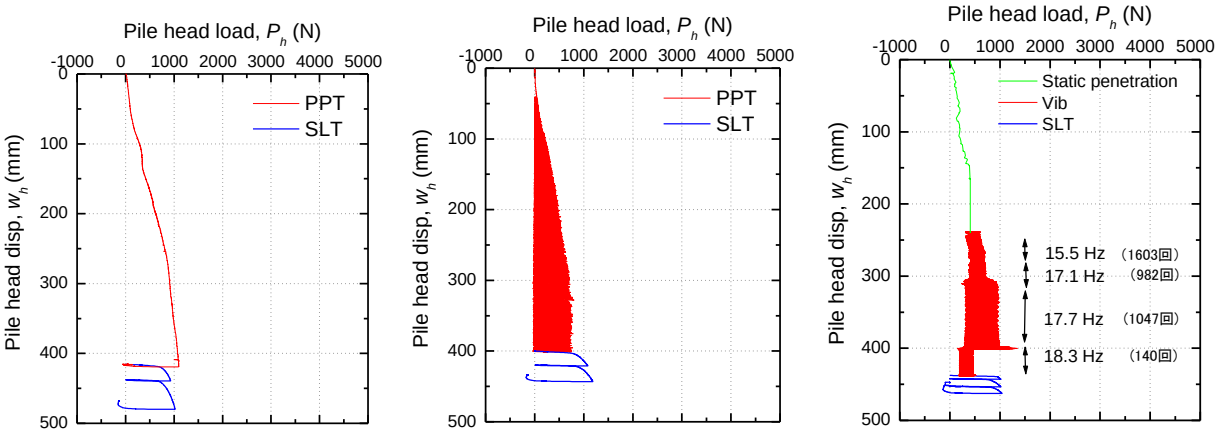

(a) Case 4 (Saturated, Push-in) **(b)** Case 5 (Saturated, Surging) **(c)** Case 6 (Saturated, Vibratory)

Fig. 10 The relationship between the pile head load, P_h, and the pile head displacement, w_h, in the case 4 to 6

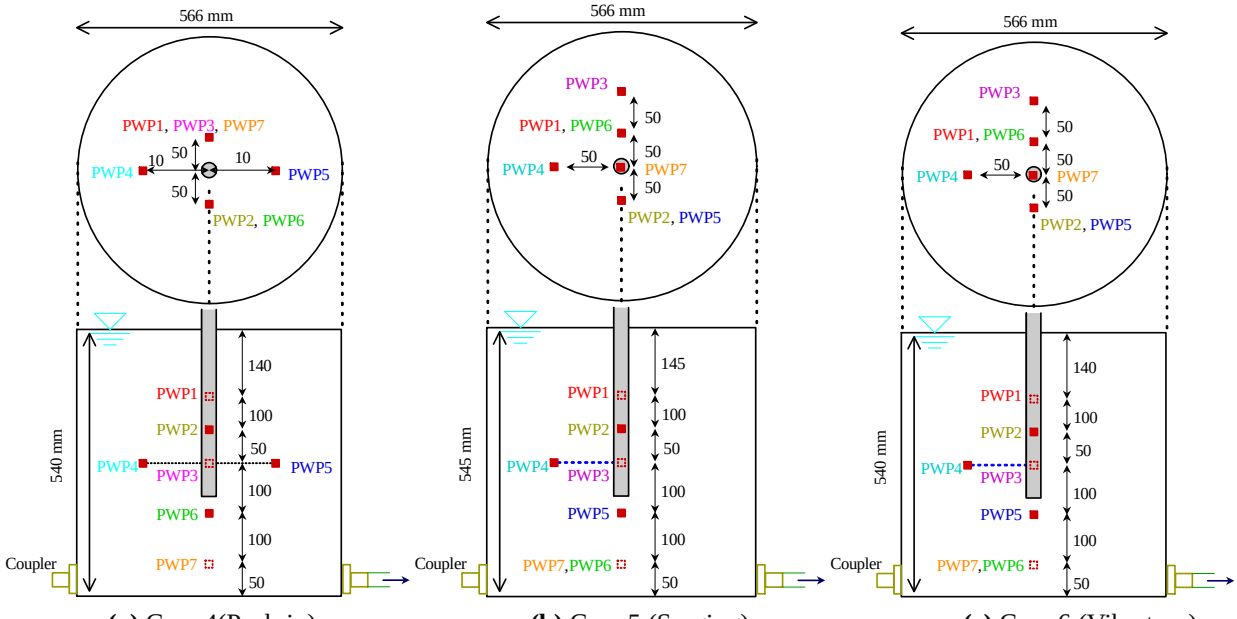

(a) Case 4(Push-in) **(b)** Case 5 (Surging) **(c)** Case 6 (Vibratory)

Fig. 11 Locations of 7 pore water pressure transducers in Cases 4 to 6

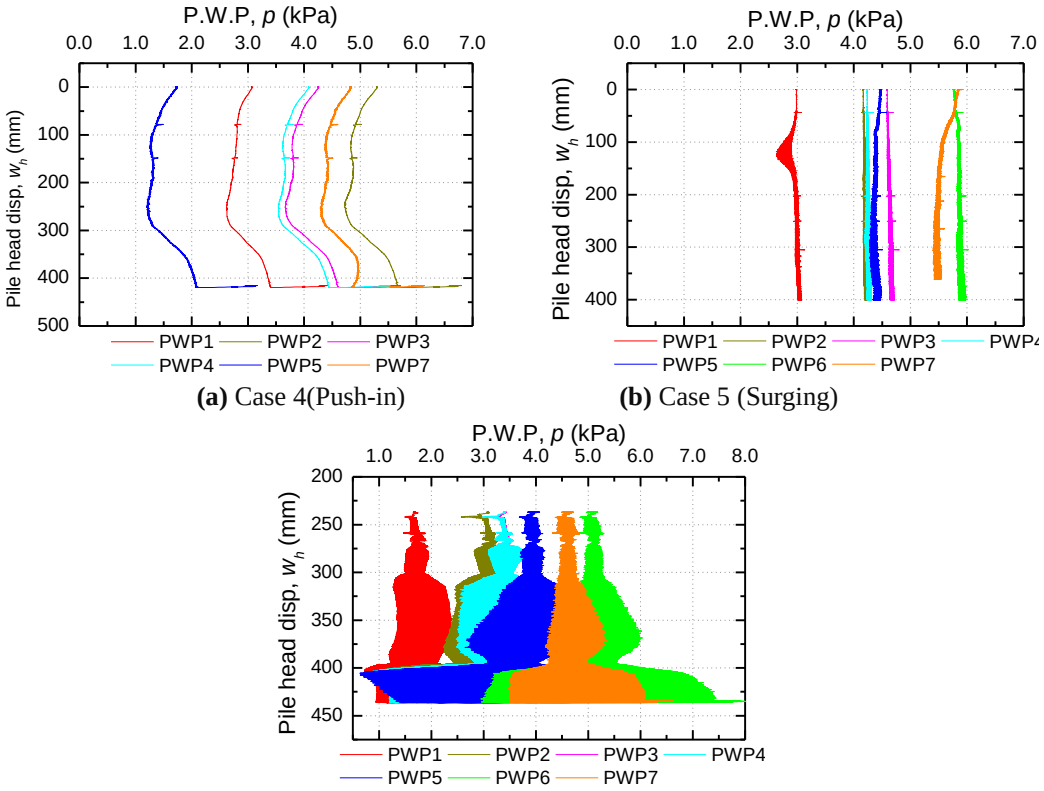

(a) Case 4(Push-in) **(b)** Case 5 (Surging)

(c) Case 6 (Vibratory)

Fig. 12 The relationship between the pile head displacement, w_h, and the water pressure (P.W.P.), p, during PPT

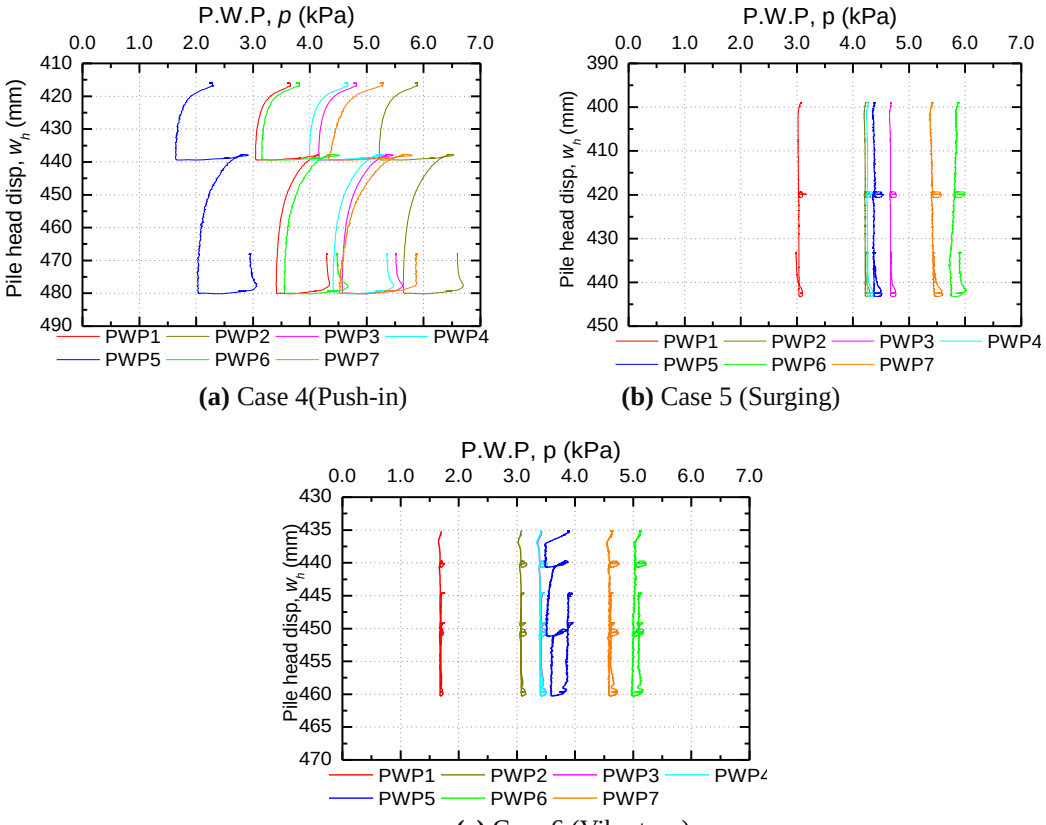

(a) Case 4(Push-in) **(b)** Case 5 (Surging)

(c) Case 6 (Vibratory)

Fig. 13 The relationship between the pile head displacement, w_h, and the water pressure (P.W.P.), p, in SLT

It is inferred from the results of the triaxial tests that larger positive pore water pressures were generated in vibratory penetration where pile penetration velocity and number of cyclic loading were higher compared to those in the surging installation. In Case 5 (surging), penetration speed of the pile was 0.2 mm/s and the total number of cyclic loading was 350, while in Case 6 (vibratory) those were 87 mm/s and 3800. Hence, P_h was smaller in vibratory penetration than in surging.

3.2. Static load test stage

Load-settlement relations in the stage of static load test (SLT) are indicated in **Fig. 9** and **Fig. 10**, respectively, for the dry and saturated ground conditions. It is seen from **Fig. 9** that P_h in all of the cases of dry ground (Cases 1 to 3) in SLT are comparable, regardless of different penetration resistance. Also in the cases of the saturated ground (Cases 4 to 6), P_h are similar, regardless of different penetration resistance (see **Fig. 10**).

Pore water pressures measured in the SLTs are shown in **Fig. 13**. As mentioned earlier, the penetration resistance of the pile in Case 6 (vibratory) just before the final penetration was largely reduced by generation of large pore water pressures. It is thought that the ground was reconsolidated (the excess pore water pressures disappeared) while the vibratory equipment was removed after PPT, resulting in the recovery of the pile capacity.

It can be seen from **Fig. 13** that changes of the pore water pressures (PWPs) in SLT in Cases 5 and 6 are smaller than those in Case 4. However, they have similar trend. Negative PWP increments were caused when the pile was loaded (compressed), and positive PWP increments were caused when the pile was unloaded to zero. When the pile was pulled-out at a rate of 0.2 mm/s after the loading cycles, negative PWP increments were caused, although the magnitudes were less compared with those generated in the loading stages. These phenomena of the PWPs are closely related to the dilatancy behaviours of the sand. As has been shown in **Fig. 7**, negative PWP was generated when the dense sand was sheared, indicating the positive dilatancy of the dense sand. It is seen from **Fig. 13** that higher degree of the positive dilatancy was caused in the SLT of Case 4 (push-in).

Here, let us discuss the results of Case 3 (**Fig. 9(c)**) again. As mentioned earlier, the pile resistance, P_h, during vibration was smaller than that in the SLT, regardless of the dry sand condition. According to Watanabe and Kusakabe (2013), excess pore air pressure is generated in dry sand when it is sheared very rapidly in the triaxial compression testing. Based on Watanabe and Kusakabe (2013) and generation of positive excess pore water pressures indicated in **Fig. 12(c)**, a possible explanation for **Fig.9(c)** is the generation of excess pore air pressure during vibration in Case 3 (dry, vibration). Of course, it is difficult to derive a definite conclusion for this at present stage. Experiments with measurements of pore air pressures would help us investigate the influence of generation of pore air pressure on pile behaviour.

Figs. 14 to **16** show again the load-settlement relations of the pile in the cases of saturated ground (Cases 4 to 6) in detail, together with the corresponding axial force distributions (axial forces at the gauge points in Fig. 1). #1 in each figure indicates the yield point in the 1st loading cycle, and #3 the yield point in the 2nd loading.

It is seen from **Fig. 14(a)** and **Fig. 15(a)** that pile head load, P_h, at #1 is similar to that at #3 in Case 4 and Case 5. It is seen from **Fig. 14(b)** and **Fig. 15(b)** that the distributions of axial forces at #1 and #3 are almost equal in Case 4 and Case 5. In contrast, it is seen from **Fig. 16(a)** that P_h at #1 is higher than that at #3 in Case 6. And the curvature at #1 is sharp.

Comparison of the axial force distributions at #1 and #3 (**Fig. 16b**) indicates that the pile tip resistances at #1 and #3 are almost equal, while the total shaft resistance at #3 is reduced from that at #1. Similar results were observed in Case 3 (dry, vibration), although figures are not shown.

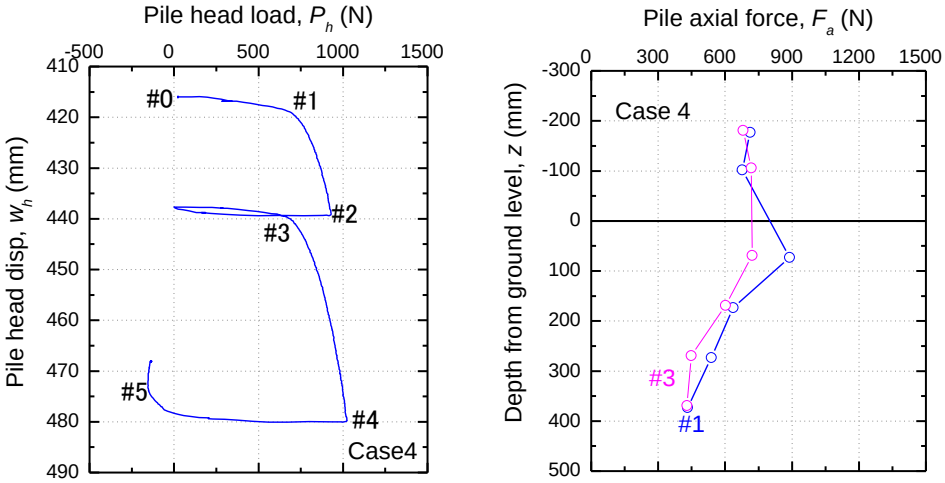

(a) SLT result **(b)** Axial force

Fig. 14 Axial force distribution (Case 4, Saturated, Push-in)

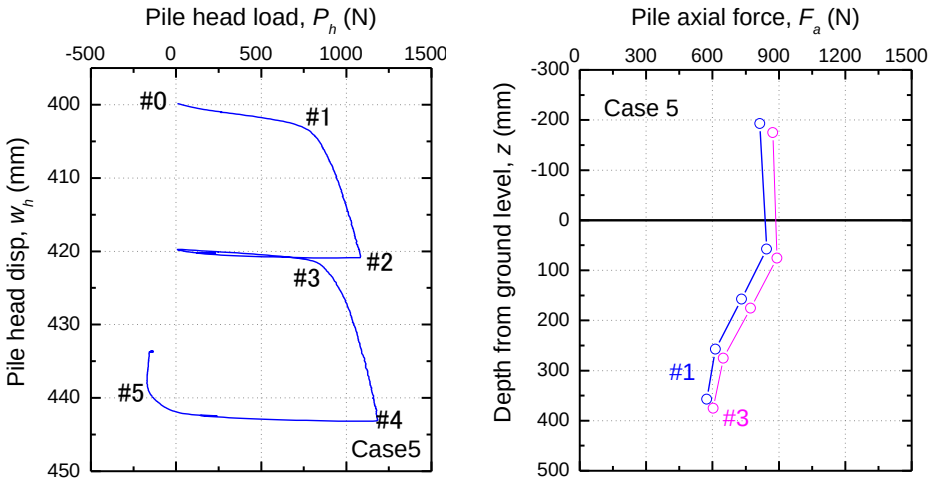

(a) SLT result **(b)** Axial force

Fig. 15 Axial force distribution (Case 5, Saturated, Surging)

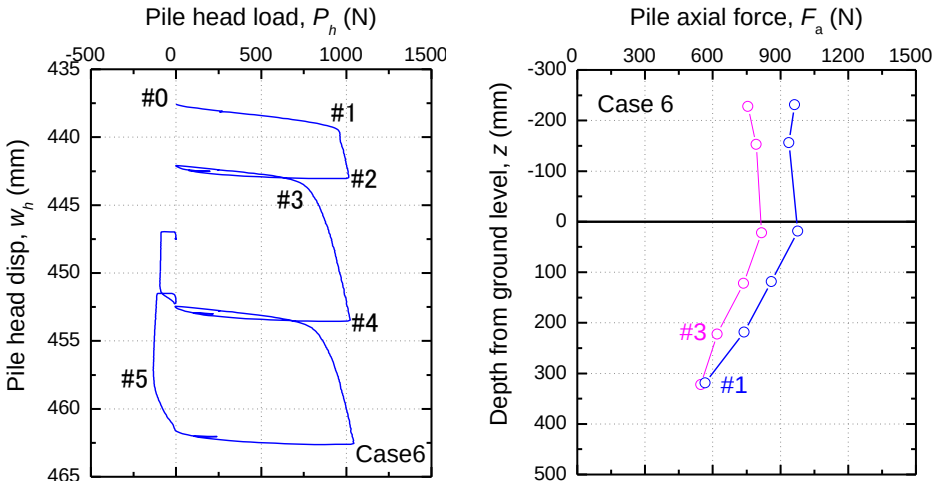

(a) SLT result **(b)** Axial force

Fig. 16 Axial force distribution (Case 6, Saturated, Vibratory)

4. Conclusion

In this paper, influences of different piling methods i.e. jack-in, surging and vibration, and the ground conditions of dry or saturated on pile behaviours were investigated through a series of model load test. Indicative findings are:

Penetration resistance of the pile penetrated by vibratory driving in dry and saturated ground was smallest in three piling methods.

In the saturated ground, as the number of cyclic loading and vibration frequency increased, positive pore water pressure was generated largely, and penetration resistance of the pile became lower.

In the dry ground, it was inferred that positive pore air pressure was generated as the number of cyclic loading and vibration frequency increase, and the penetration resistance of the pile become lower even in the dry ground condition.

6. References

Moriyasu S., Meguro H., Matsumoto T., Kobayashi S., Shimono S. 2016. Influence of surging and jack-in pile installation methods on pile performance observed in model load tests in dry sand grounds. Proceedings of 19SEAGC, Kuala Lumpur, Malaysia, pp. 621-626.

Watanabe, K. and Kusakabe, O. 2013. Reappraisal of Loading Rate Effects on Sand Behaviour in View of Seismic Design for Pile Foundations. Soils and Foundations, 53 (2), pp. 215-231.